Convergent evidence for global processing of shape

Robert J. Green School of Psychological Science, The University of Western Australia, Perth, Australia

J. Edwin Dickinson School of Psychological Science, The University of Western Australia, Perth, Australia

David R. Badcock School of Psychological Science, The University of Western Australia, Perth, Australia

There is an ongoing debate over whether there is convincing evidence in support of global contour integration in shape discrimination tasks, particularly when using radial frequency (RF) patterns as stimuli (Baldwin, Schmidtmann, Kingdom, & Hess, 2016). The objection lies in the previous use of high-threshold theory (HTT), rather than signal detection theory (SDT) to model the probability summation estimates of observer thresholds to determine whether integration of information is occurring around the contour. Here we used a discrimination at threshold method to establish evidence of global processing of two frequently used RF patterns (RF3 and RF5) that does not require mathematical modeling. To provide a bridge between current and past research we examined the two proposed methods, finding that HTT produced probability summation estimates that were more conservative than SDT (when an appropriate number of channels was used to generate estimates). We found no difference in observer thresholds when an RF pattern was presented as the only test stimulus in a block of trials or when two RF patterns were interleaved, and no evidence for a decrease in psychometric slopes with increasing numbers of stimulus elements. These findings are contrary to what is predicted by SDT for a stimulus whose detection conforms to probability summation. Therefore, our results find no evidence that supports probability summation, further demonstrating the importance of using random phase RF patterns while measuring integration around a contour and providing strong evidence for global shape processing around low frequency RF patterns.

Introduction

One important function of the visual system is the identification of shapes within the visual field so that appropriate actions can be taken. Construction of a global representation of simple shapes is thought to be first achieved in lateral occipital areas (Vernon, Gouws, Lawrence, Wade, & Morland, 2016) by the combination of information from local responses to the image earlier in the visual stream (Van Essen, Anderson, & Felleman, 1992; Vernon et al., 2016). Global shape processing, in our case based on the integration of local information around the shape's contour, can aid in the detection and discrimination of different shapes. This has been examined by numerous previous studies using radial frequency (RF) patterns (Almeida, Dickinson, Maybery, Badcock, & Badcock, 2013; Almeida, Dickinson, Maybery, Badcock, & Badcock, 2014; Baldwin et al., 2016; Bell, Badcock, Wilson, & Wilkinson, 2007; Bell, Dickinson, & Badcock, 2008; Dickinson, Han, Bell, & Badcock, 2010; Green, Dickinson, & Badcock, 2018a, 2018b; Loffler, Wilson, & Wilkinson, 2003; Schmidtmann, Kennedy, Orbach, & Loffler, 2012; Wilkinson, Wilson, & Habak, 1998; Wilson & Propp, 2015). RF patterns are derived from circles by sinusoidally modulating their radius as a function of the polar angle. They are defined by their RF number (the number of wavelengths (ω) it takes to complete 360°) and the number of cycles (the number of wavelengths actually incorporated into the otherwise circular pattern; see Figure 1). Adjusting the amplitude of the sine wave used to modulate the circle adjusts the salience of deformation, resulting in an object stimulus parameter that is suitable for deformation-threshold estimation. In the initial paper describing RF patterns, Wilkinson et al. (1998) found subjects had sensitivity to radial deformations as small as 2–4′ of visual angle. This distance is smaller than the center-to-center separation between photoreceptors in the human fovea (approximately 36′ Westheimer, 2010).

In the past, researchers have examined global processing of shapes by comparing observed thresholds

Citation: Green, R. J., Dickinson, J. E., & Badcock, D. R. (2018). Convergent evidence for global processing of shape. *Journal of Vision*, *18*(7):7, 1–15, https://doi.org/10.1167/18.7.7.

https://doi.org/10.1167/18.7.7 Received August 25, 2017; published July 18, 2018 ISSN 1534-7362

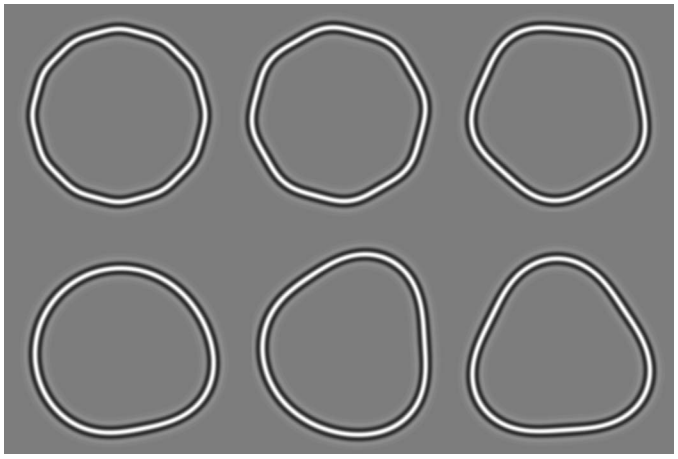

Figure 1. Anticlockwise from bottom left: RF3(1), RF3(2), RF3, RF5, RF8, and RF12. All patterns have their amplitude defined by the same equation $1/(1+\omega^2)$, where ω is the RF number and results in a pattern well above threshold levels, but shown for illustrative purposes. Changing the RF number changes the polar angle separating lobes on successive cycles at amplitude maxima (angle subtended at the center of the pattern by adjacent points of maximum curvature), while changing the number of cycles (and changing the amplitude) changes the amount of signal present.

to those predicted by an estimation of probability summation assuming local processing (Almeida et al., 2014; Dickinson et al., 2010; Loffler et al., 2003; Schmidtmann et al., 2012; Tan, Dickinson, & Badcock, 2013). Probability summation is the increased likelihood of detecting a single local deformation as the number of elements (cycles, or repetitions of the local information) increase. If thresholds decrease significantly faster, when more cycles are added, than predicted by probability summation, there is evidence for global processing occurring. Prior researchers have presented evidence for global processing of patterns up to RF10 but suggest local processing (probability summation) occurs for higher numbered RF patterns (Loffler et al., 2003).

The technique of probability summation estimation used in the majority of these studies of RF patterns was introduced by Loffler et al. (2003) and modeled under the framework of high-threshold theory (HTT; Quick, 1974; Wilson, 1980). Recent work has noted previous rejection of HTT as a general theory of threshold detection (Baldwin et al., 2016; Kingdom, Baldwin, & Schmidtmann, 2015; Schmidtmann, Jennings, Bell, & Kingdom, 2015; Schmidtmann et al., 2012) and suggested that signal detection theory (SDT) is a better framework to use for generating probability summation estimates. Baldwin et al. (2016) collected data for the detection of single modulation cycles and created receiver operating characteristic curves that provided compelling evidence against the use of HTT and modeled a number of different SDT probability summation estimates; however, their observer thresholds were not significantly different to either their probability summation estimates or their additive summation estimates (summing of individual component estimates by a mechanism sensitive to the compound stimulus). Neither were they able to discriminate between probability summation and additive summation predictions using their methods. Although this raises the question of whether incorrect conclusions have been reached by using either method, other techniques have provided evidence for global processing of low frequency RF patterns (e.g., parallel processing in visual search: Almeida, Dickinson, Maybery, Badcock, & Badcock, 2010a, 2010b; Dickinson, Haley, Bowden, & Badcock, 2018; independent processing of low and high RFs at deformation threshold: Bell et al., 2007; Dickinson, Cribb, Riddell, & Badcock, 2015; and pattern indentification at deformation-detection threshold: Dickinson, Bell, & Badcock, 2013), and there is also evidence that the methodology employed by Baldwin et al. (2016) may have led to their inability to reject probability summation (see Green et al., 2017; Green, Dickinson, & Badcock, 2018b).

However, there is still currently some confusion about whether global processing occurs for RF patterns above RF3. This has prompted the authors of the current paper to reinvestigate whether there is evidence for global processing of an RF3 (a pattern that Baldwin et al., 2016 agrees demonstrates evidence of global processing) and an RF5 (a pattern with a higher frequency than the RF4 used by Baldwin et al., 2016, and therefore, should result in integration that is poorer than an RF4; Wilkinson et al., 1998). By comparing the pattern of results we can determine whether there is a difference in the way an RF3 is processed compared to other low frequency RF patterns.

Using a discrimination at threshold task, we will first determine whether there is evidence that RF3 and RF5 patterns are detected in discrete information channels (Watson & Robson, 1981). We will use the RF patterns to compare their detection thresholds to the thresholds required to discriminate between them in the same observers. If, following Watson and Robson (1981), as past researchers have suggested (Dickinson et al., 2015; Graham, 1989; Dickinson et al., 2013; Watson & Robson, 1981), we are able to discriminate between RF patterns at the same threshold required for their detection, then this will be evidence of independent processing based on global shape information. This is because to discriminate between patterns requires a global judgment of shape.

This global shape judgment requires, at minimum, the combining of information at two separate corners on the shape's contour and is, therefore, evidence of

integration of information around the contour. If there is integration of information around the shape's contour at threshold for detection, then there is global processing occurring at detection threshold. Dickinson et al. (2013) found that the local difference in presentations of an RF3 and RF6, each containing only a single cycle, was not sufficient to discriminate between these patterns at their threshold for detection and that two cycles or more of modulation were required on each pattern for discrimination to be achieved.

Schmidtmann et al. (2012) suggested that incomplete RF patterns (i.e., an RF pattern that has a portion of the contour conforming to a circle) demonstrate improvements in threshold, which can be explained by probability summation. Only when the complete RF pattern is viewed (i.e., all cycles of modulation are present) does integration of information occur around the contour. Therefore, by using a discrimination at threshold task for each possible number of cycles of modulation of an RF3 and RF5, we will be able to directly test this assertion. If observers are able to discriminate between incomplete RF patterns at their threshold for detection, it will provide strong evidence against integration only occurring for complete RF patterns as Schmidtmann et al. (2012) have suggested.

This paper will investigate whether there is evidence of global processing for RF3 and RF5 patterns; two patterns with previously strong evidence for global integration but that may differ in their ability to reject probability summation using SDT due to their different strengths of integration around the contour. We will then use the data collected to analyze whether SDT estimates of probability summation can indicate the presence of global processing and how these differ from HTT estimates. Given the majority of previous research has used HTT and either an RF3 or RF5 to examine global processing around the contour of RF patterns (see appendix A of Baldwin et al., 2016), the inclusion of HTT and SDT estimates allow the evaluation of the suggestion by Baldwin et al. (2016) that incorrect conclusions may have been reached by previous researchers.

While some of these issues have been investigated by Dickinson, Bell, and Badcock (2013) and Green et al. (2017), the purpose of this manuscript is to: (a) test whether there is a difference in the processing of RF3 and RF5 patterns; (b) directly test the assertion that integration only occurs around complete RF patterns as suggested by Schmidtmann et al. (2012); and (c) examine additive summation estimates from SDT, along with probability summation estimates generated when modeled using SDT and HTT for two different RF patterns and determine whether these agree with the evidence for integration provided by the discrimination at threshold task.

Methods

Observers

Two of the authors and two naive observers participated in the current study after giving informed consent. All subjects had normal or corrected-to-normal visual acuity, which was assessed using a LogMAR chart. ED has a divergent squint and used a black opaque occluder (eye patch) to cover his left eye during testing. The research protocol was approved by the University of Western Australia human ethics committee and conforms to the Declaration of Helsinki.

Stimuli

The stimuli used were RF patterns following Wilkinson et al. (1998). An RF pattern is a deformed circular contour with the radius modulated by:

$$R(\theta) = R_0 \times (1 + A.\sin(\omega\theta + \varphi)) \quad (1)$$

where θ is the angle created with the x-axis, R_0 is the mean radius (1° of visual angle in all conditions), A is the amplitude of modulation (proportion of mean radius), ω is the frequency of modulation (number of cycles per 2π radians) and φ is the phase of the sinusoidal modulation. A first derivative of a Gaussian (D1) was used to ensure a smooth transition between modulated sectors and unmodulated sectors, replacing the first half and last half cycles of the train of modulation, as also employed by Loffler et al. (2003). Therefore, at one cycle, the modulated sector conforms solely to a D1, with a maximum gradient identical to that of a sine wave with the same amplitude (Loffler et al., 2003). Additional cycles were always added adjacent to other cycles of modulation to maintain the polar angle between adjacent points of maximum curvature (corners) of the RF pattern, a feature shown to be important in the perception of RF patterns (Dickinson et al., 2015; Dickinson et al., 2013). The cross section of the luminance profile of the path conformed to a fourth derivative of a Gaussian (D4) with a frequency spectrum peaking at 8 c/° ($f_{peak} = \sqrt{2}/\pi\sigma$; equation 2 from Wilkinson et al., 1998) resulting from sigma (σ) of 3.376′ of visual angle.

Apparatus

Stimuli were generated using a PC (Pentium 4, 3 GHz) and custom software written in MATLAB 7.0.4 (MathWorks, Natick, MA). The observers viewed a Sony Trinitron G520 monitor (100-Hz refresh rate),

which presented the stimuli from the frame buffer of a ViSaGe (Cambridge Research Systems, Rochester, UK) visual stimulus generator. Screen resolution was 1,024 × 768 pixels and viewing distance was stabilized at a distance of 65.5 cm using a chinrest, which resulted in each pixel subtending a visual angle of 2′. An Optical OP 200-E photometer (head model number 265) was used to linearize the luminance response and to calibrate background luminance to 45 cd/m^2 and maximum luminance to 90 cd/m^2, resulting in a Weber contrast of 1. Responses were signaled using the left and right buttons of a Cambridge Research Systems CB6 button box. A square fixation point (6′ side length) was used to indicate the center of the screen, where stimuli were presented, with the center of each pattern able to vary ±6′ of visual angle in the horizontal and vertical directions, randomly selected on a trial by trial basis.

Procedure

A two-interval forced-choice paradigm was used for all three conditions, with a reference stimulus in one interval which consisted of a circle ($A = 0$ in Equation 1), and a test stimulus, either an RF3 with one, two, or three cycles of modulation or an RF5 with one, two, three, four, or five cycles of modulation, in the other interval. The order of presentation was randomized between trials. Each stimulus was presented for 160 ms, with a 300-ms interstimulus interval, as used in previous similar studies employing RF patterns (Bell et al., 2007; Bell et al., 2008; Dickinson et al., 2013). In the first condition (1RF detection), observers reported which interval (first or second) contained the pattern that appeared most deformed from circular. Within a block of trials only one RF pattern, with a fixed number of cycles, was presented (e.g., only an RF3 with two cycles of modulation). In the second condition (2RF detection), observers again reported which interval contained the pattern most deformed from circular; however, a block of trials contained both RF patterns on different trials (one interval containing a circle, the other containing either an RF3 or RF5) but with the same number of cycles where possible, resulting in the following pairings: RF3(1) and RF5(1); RF3(2) and RF5(2); RF3(3) and RF5(3); RF3(3) and RF5(4); and RF3(3) and RF5(5). The third condition (2RF discrimination) was presented in the same way as 2RF detection; however, observers reported which pattern was displayed in either interval (i.e., the response was RF3 or RF5). Trials were presented using the method of constant stimuli, sampling nine amplitudes of modulation, with 60 trials per amplitude spread over three separate blocks each containing 180 trials.

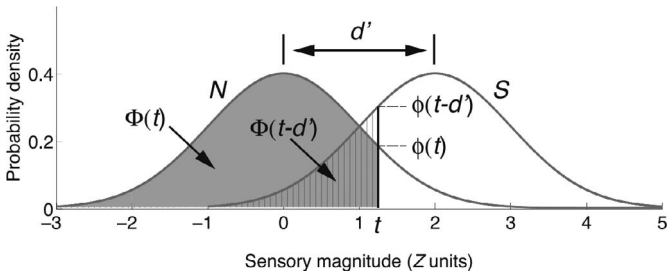

Figure 2. Parameters for calculating probability summation under SDT, from Kingdom et al. (2015).

Observers randomly interleaved the different blocks of 1RF detection (to help determine the appropriate method of constant stimuli step size to use) then randomly interleaved the blocks from 2RF detection and 2RF discrimination. To generate the HTT probability summation prediction for the conditions, a Quick function (Quick, 1974) was fit to the data as follows:

$$p(A) = 1 - 2^{-\left(1+(A/\alpha)^{\beta}\right)} \quad (2)$$

where p is the probability of correct response, A is the amplitude of modulation as a proportion of the radius on an unmodulated circle, α is the threshold at the 75% correct response level and β controls the slope of the psychometric function. Probability summation slope (threshold as a function of number of cycles of modulation) under HTT is estimated by $1/\bar{\beta}$, where $\bar{\beta}$ is the average of the slopes of the psychometric functions for all cycles of the RF pattern (Wilson, 1980). To determine the SDT estimate of probability summation, d prime (d') was estimated using:

$$d' = (gA)^{\tau} \quad (3)$$

where d' is the internal strength of a signal, g is a scaling factor incorporating the reciprocal of the internal noise standard deviation, A is the stimulus intensity, and τ is the exponent of the internal transducer (relationship between stimulus intensity and perceptual salience). Figure 2 illustrates the signal and noise distributions under SDT.

The estimated proportion correct for probability summation under SDT was given by Kingdom et al. (2015):

$$Pc = n\int_{-\infty}^{\infty}\phi(t-d')\Phi(t)^{QM-n}\Phi(t-d')^{n-1}dt\ldots + (Q-n)\int_{-\infty}^{\infty}\phi(t)\Phi(t)^{QM-n-1}\Phi(t-d')^{n}dt \quad (4)$$

where Pc is the proportion correct and set at 0.75, t is sample stimulus strength, the heights of the noise and signal distributions at t are given by $\phi(t)$ and $\phi(t-d')$, the areas under the noise and signal distributions to the

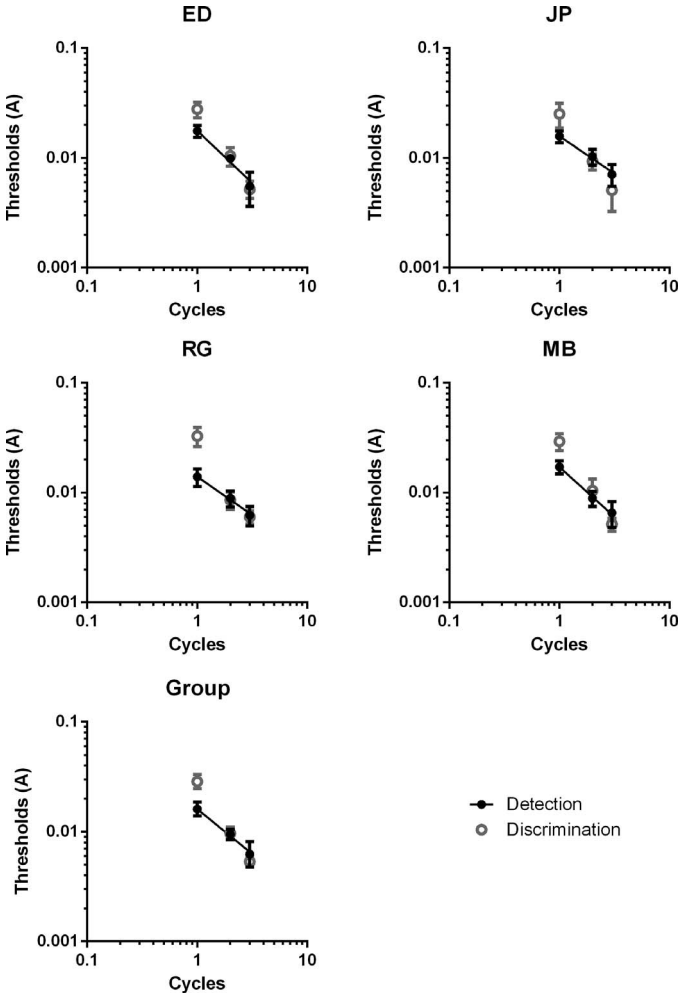

Figure 3. RF3 detection (black solid circles) and discrimination (gray open circles) thresholds for all four observers (top and middle) and average of those observers (bottom left), error bars represent 95% CIs. Detection thresholds are fitted using a power function (black solid line). Note for one cycle, discrimination thresholds appear to be greater than detection thresholds, this does not appear to be the case for two or three cycles.

left of t are $\Phi(t)$ and $\Phi(t - d')$ respectively, Q is the number of monitored channels within the perceptual system, M is the number of alternatives in the forced choice task, and n is the number of stimulus components or local cues. This equation is implemented in the Palamedes toolbox, version 1.8.1 (Prins & Kingdom, 2009, downloaded in 2016 from http://www.palamedestoolbox.org).

Results

Using the Quick function (Equation 2), estimates of 75% correct detection and discrimination thresholds were calculated for all conditions. Figure 3 shows the discrimination (gray open circles) and detection (black filled circles) thresholds for each of the four observers individually and also the averaged results, when the target was an RF3 that varied in the number of cycles presented on the otherwise circular contour. Note, the conditions were 1RF detection, discrimination of a single RF pattern (e.g., RF3[2]) and a circle; 2RF detection, again discrimination of an RF pattern and a circle, however, RF3 and RF5 stimuli were interleaved; and 2RF discrimination, discrimination of RF3 and RF5 stimuli.

RF3 data analysis

A repeated-measures 2 (detection, discrimination) × 3 (1 cycle, 2 cycles, 3 cycles) factorial analysis of variance (ANOVA) examined the effect of both number of cycles and condition (2RF detection or 2RF discrimination) on thresholds. There was a significant main effect of both condition, $F(1, 3) = 24.31$, $p = 0.02$, $\eta_p^2 = 0.89$, and cycles, $F(2, 6) = 284.21$, $p < 0.001$, $\eta_p^2 = 0.99$. There was also a significant interaction, $F(2, 6) = 34.12$, $p = 0.001$, $\eta_p^2 = 0.92$. Visual inspection of the data and the significant interaction prompted the investigation of differences between discrimination and detection thresholds. Bonferroni-adjusted, paired-samples t tests revealed discrimination thresholds were significantly greater than detection thresholds at one cycle ($p < 0.05$), but there were no significant differences between discrimination and detection thresholds at two or three cycles ($ps > 0.05$). Bonferroni-adjusted, paired-samples t tests also showed a significant difference between all numbers of cycles (all $ps < 0.05$).

Within SDT the number of channels being monitored (Q in Equation 4) is important in both probability summation and additive summation calculations. As shown in Kingdom et al. (2015), increasing the number of channels increases the predicted threshold using a SDT probability summation model. The effect of increasing the number of channels (Q) is greatest at low numbers and if we assume the number of channels monitored is equal to either the number of lobes on the RF pattern (although this is unlikely to be correct for random phase patterns where many locations need to be monitored) or a common local feature (e.g., point of maximum convexity), we would expect to see a systematic increase in detection thresholds of the 2RF detection condition compared to the 1RF detection condition due to the monitoring of either eight (three channels from the RF3 plus five channels from the RF5) or five channels (only the larger number of five channels is required) instead of three.

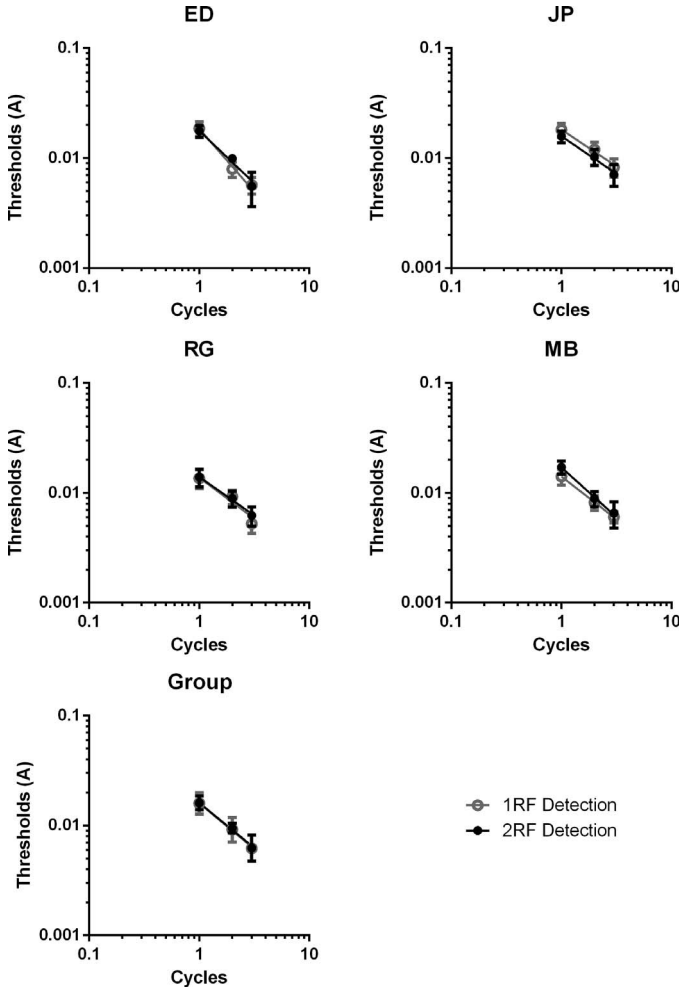

Figure 4. Detection thresholds for all four observers and their averaged results for an RF3 presented as the only possible stimulus in a block (1RF detection; gray open circles) and presented with an RF5 as another possible test stimulus within a block (2RF detection; black solid circle). A power function (solid black line) with a slope of −0.82 fits both data sets for the grouped results ($R^2 > 0.99$ for both data sets).

To examine the effect of number of stimuli presented within a block on thresholds a repeated-measures 2 (1 RF pattern, 2 RF patterns) × 3 (1 cycle, 2 cycles, 3 cycles) factorial ANOVA was used. Figure 4 shows the thresholds averaged across the four observers. There was a significant main effect of number of cycles, $F(2, 6) = 66.78$, $p < 0.001$, $\eta_p^2 = 0.96$, but not for number of stimuli, $F(1, 3) = 0.01$, $p = 0.93$, $\eta_p^2 = 0.003$. There was also no interaction effect, $F(2, 6) = 0.02$, $p = 0.99$, $\eta_p^2 = 0.01$. It is clear there is no difference between the two tasks in our data and this provides evidence against the number of channels being a low value (e.g., the RF number). It suggests that for random phase patterns either the number of channels is the same for both RF patterns (e.g., the number of simple oriented V1 receptive fields falling on the contour, as random phase can result in deformation occurring at any location), or that the number of channels being monitored is so large for a single RF pattern that increasing the number of potentially relevant channels by adding another pattern has a negligible effect.

Further investigation of the effect of the partner stimulus was also conducted. As described above for the 2RF detection task, the RF5(3), RF5(4), and RF5(5) were all partnered with an RF3(3). As can be seen from the 95% confidence intervals (CIs) in Figure 5 there was no effect of the partner stimulus on detection thresholds for an RF3(3). Statistical analysis using a one-way repeated-measures ANOVA also returned no significant difference in the RF3(3) thresholds, $F(2, 6) = 0.16$, $p = 0.86$, $\eta_p^2 = 0.05$. This provides further evidence for the number of channels being equal or sufficiently large that it does not substantially affect observer thresholds.

RF5 data analysis

The same statistical analyses used for the RF3 were used to examine the data collected for the RF5. Figure 6 shows the detection (2RF detection) and discrimination (2RF discrimination) thresholds for all observers for an RF5 and their averaged results. As with the RF3, there was a significant main effect of both condition $F(1, 3) = 14.46$, $p = 0.03$, $\eta_p^2 = 0.83$, and cycles, $F(4, 12) = 204.36$, $p < 0.001$, $\eta_p^2 = 0.99$. There was also a significant interaction effect, $F(4, 12) = 26.10$, $p < 0.001$, $\eta_p^2 = 0.90$. Bonferroni-adjusted, paired-samples t tests were again used to examine the difference in thresholds between discrimination and detection conditions. Discrimination thresholds were significantly greater than detection thresholds at one cycle ($p < 0.05$), but there were no significant differences between discrimination and detection thresholds at two, three, four, or five cycles ($ps > 0.05$). Bonferroni-adjusted, paired-samples t tests showed a significant difference between all numbers of cycles (all $ps < 0.05$).

The effect of number of stimuli presented within a block was examined (i.e., 1RF detection compared to 2RF detection). Figure 7 shows the thresholds averaged across the four observers for an RF5 presented as the only test stimulus in a block of trials (1RF detection) and thresholds when it was presented with an RF3 interleaved (2RF detection). Again, similar to the RF3 data, there was a significant main effect of number of cycles, $F(4, 12) = 133.94$, $p < 0.001$, $\eta_p^2 = 0.98$, but no significant main effect of number of stimuli, $F(1, 3) = 1.27$, $p = 0.34$, $\eta_p^2 = 0.30$, and no interaction effect, $F(4, 12) = 0.71$, $p = 0.60$, $\eta_p^2 = 0.19$. The data demonstrates equivalent thresholds for these two conditions at every number of cycles and, therefore, having an RF3 within

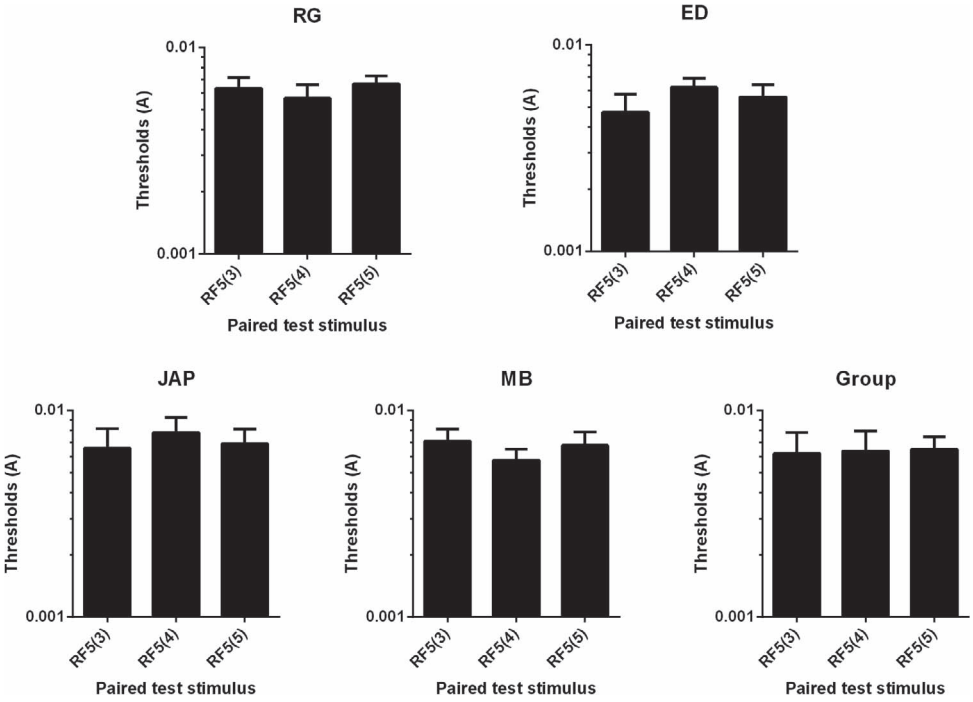

Figure 5. Detection thresholds for an RF3 at three cycles of modulation for all observers with 95% CIs, and the averaged thresholds (bottom right). The *x*-axis shows the other test stimulus that was presented within the same block of trials, an RF5 at three cycles RF5(3), four cycles RF5(4), and five cycles RF5(5) of modulation.

the same block of trials as an RF5 has no measureable effect on its thresholds for detection.

Psychometric slopes

SDT predicts that for thresholds conforming to probability summation in a fixed attention window scenario, the slope of the psychometric functions should become shallower with increasing number of stimulus components (Kingdom et al., 2015; Pelli, 1985). We tested the psychometric slopes of the RF3 using a 3 (1RF detection, 2RF detection, 2RF discrimination) × 3 (1 cycle, 2 cycles, 3 cycles) repeated-measures ANOVA. There was no significant main effect of either condition, $F(2, 6) = 5.00$, $p = 0.053$, Psychometric slopes = 0.63, or number of cycles $F(2, 6) = 0.72$, $p = 0.53$, $\eta_p^2 = 0.19$. There was also no significant interaction effect, $F(4, 12) = 2.42$, $p = 0.11$, $\eta_p^2 = 0.45$. Linear trend analysis of the effect of number of cycles on the psychometric slope was also not significant $F(1, 3) = 0.66$, $p = 0.48$, $\eta_p^2 = 0.18$. Visual inspection of the data (see Figure 8) would indicate there is no consistent pattern of change in the psychometric slopes.

The same method was used to examine the RF5 data. A 3 (1RF detection, 2RF detection, 2RF discrimination) × 5 (1 cycle, 2 cycles, 3 cycles, 4 cycles, 5 cycles) repeated-measures ANOVA was used. There was a significant main effect of cycles, $F(4, 12) = 4.61$, $p = 0.02$, $\eta_p^2 = 0.61$, but no significant main effect of condition, $F(2, 6) = 0.63$, $p = 0.57$, $\eta_p^2 = 0.17$, and no significant interaction effect, $F(8, 24) = 1.03$, $p = 0.45$, $\eta_p^2 = 0.23$. Pairwise comparisons indicated psychometric slopes at one cycle of modulation were significantly less than at four and five cycles of modulation, and that the slope at two cycles of modulation was significantly higher than three cycles of modulation. No other differences were found. Linear trend analysis of the effect of number of cycles on psychometric slopes was also not significant, $F(1, 3) = 8.70$, $p = 0.06$, $\eta_p^2 = 0.74$. If the linear trend was significant it would suggest psychometric slopes are trending upwards (steeper), the opposite of that predicted by SDT probability summation. However, it is clear from visual inspection of the data (Figure 9) that there again appears to be no real pattern. Much more extensive data collection may have reduced the variability in the data allowing greater sensitivity to changes in the slope of the psychometric function but the current data do not suggest the extra time would be usefully spent.

High threshold theory

Both HTT and SDT provide probability summation slope estimates, a prediction for the index of threshold as a function of the number of cycles of modulation

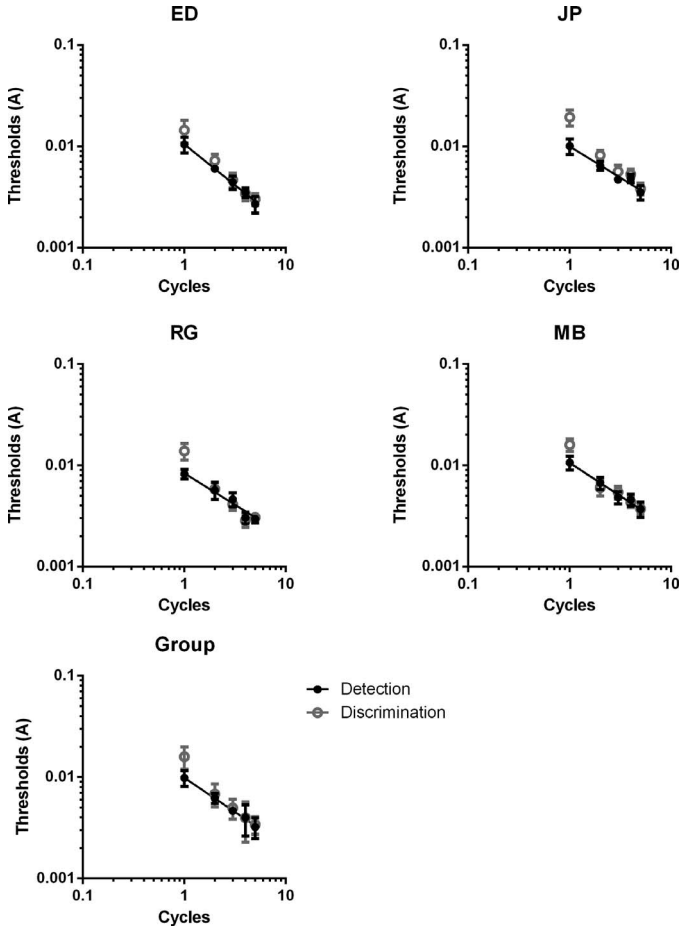

Figure 6. Detection (black solid circles) and discrimination (gray open circles) thresholds with 95% CIs for an RF5 at one, two, three, four, and five cycles of modulation. Detection thresholds are fitted with a power function (black solid line). Note, discrimination thresholds appear to be higher than detection thresholds at one cycle of modulation.

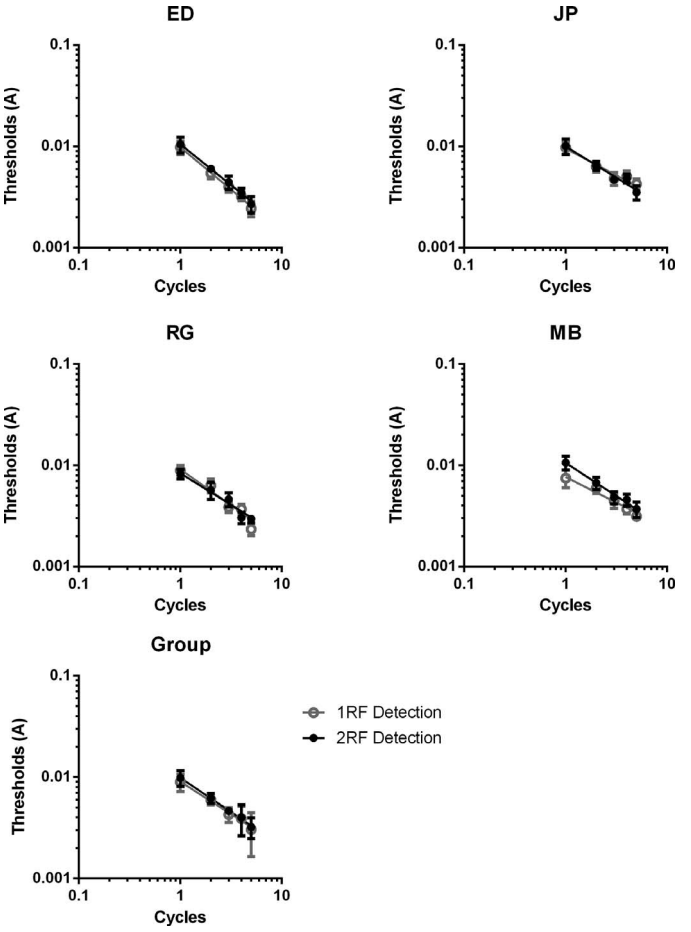

Figure 7. Detection thresholds for all four observers along with their averaged results for an RF5 when it is the only test stimulus within a block of trials (1RF detection; gray open circles) and when it is paired with an RF3 (2RF detection; black solid circle). A power function (solid black line) with a slope of −0.67 fits both data sets for the grouped results ($R^2 = 0.99$ for both data sets).

when fitted by a power function. Modeled under HTT, the slope of this line is predicted by $1/\bar{\beta}$, where $\bar{\beta}$ is the average slope of all the psychometric functions measured for the RF pattern (Equation 2). This was done for each observer and compared to the slope estimate from the power function fitted to their detection thresholds using a paired-samples t test. For the RF3, the detection slope ($M = -0.81$, 95% CI [−0.59, −1.03]) was significantly steeper than the probability summation slope ($M = -0.47$, 95% CI [−0.34, −0.60]), $t(3) = 3.31$, $p = 0.045$, $d = 1.66$. For the RF5, the detection slope ($M = -0.68$, 95% CI [−0.53, −0.82]) was also significantly steeper than the probability summation slope ($M = -0.44$, 95% CI [−0.39, −0.49]), $t(3) = 4.36$, $p = 0.022$, $d = 2.18$. Figure 10 shows the group detection thresholds and probability summation estimate averaged across four observers for both the RF3 (left) and RF5 (right).

Signal detection theory

The calculations used to estimate percentage correct for probability summation (Equation 4) within SDT rely on a number of parameters as previously outlined. d' was calculated using PAL_SDT_2AFC_PCtoDP from the Palamedes toolbox (Kingdom & Prins, 2010), estimates of g and τ were derived from the best least squares fit of Equation 3 to each observer's data. This single pair of parameters was then used in the SDT summation calculations for that observer. M was set to 2 (number of intervals presented); however, the two parameters Q (number of channels being monitored) and n (number of local elements) are less easily specified. For the probability summation formula $n \leq Q$; therefore, for an RF3, the minimum number of channels would need to be 3 with number of local elements being equal to number of cycles. It is also

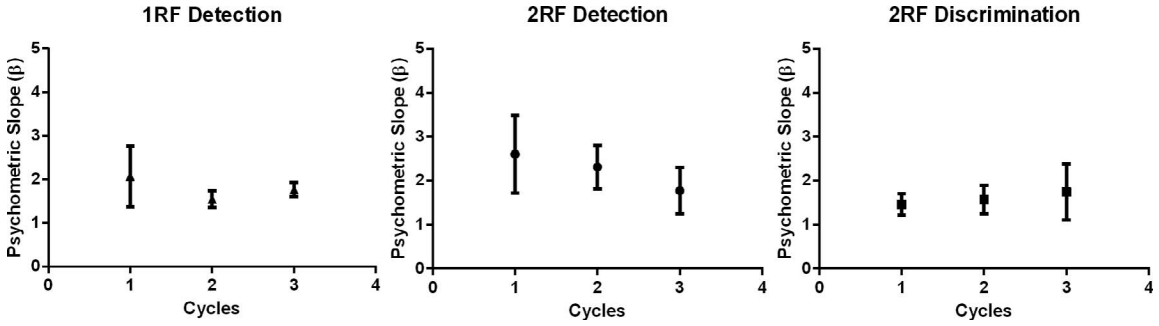

Figure 8. Average psychometric slopes of all four observers with 95% CIs across the three conditions. There appears to be no consistent pattern across the data, contrary to SDT probability summation predictions.

possible that each cycle of an RF pattern provides two cues, as Dickinson, McGinty, Webster, and Badcock (2012) found evidence for maximum orientation deviation from circular to be a critical feature and this occurs twice a cycle. Therefore, an RF3 would need a minimum of six channels, with the number of local elements equal to twice the number of cycles. The phase of the RF pattern is also likely to have an effect on the number of channels being monitored. If phases are fixed then it is reasonable to match the number of monitored local channels to the number of cycles, or to just use one cycle, since observers could know where the critical local information will occur on each trial, but random phases were employed in this study meaning that observers could not reliably predict the location of any contour feature from trial to trial. Since the cue proposed as critical by Dickinson et al. (2012) is very restricted in area, a conservative estimate is one channel per degree of phase (which results in a separation of 1′ of visual angle, the limit of two-point acuity; Westheimer, 1976), thus an RF3(3) would have 120 channels (as an RF3[3] would be identical to the same pattern rotated 120°) and an RF5(5) would have 72 channels. Thus, we had four probability summation estimates: $n =$ cycles and $Q =$ RF number; $n = 2\times$ cycles and $Q = 2\times$ RF number; $n =$ cycles and $Q = 360/\text{RF}$ number; and $n = 2\times$ cycles and $Q = 360/\text{RF}$ number.

A paired-samples t test was used to compare the detection threshold slope with each of the four SDT estimates of probability summation. Table 1 shows the results for both RF3 and RF5 data. Note that for the RF5, p values are nonsignificant for the lower numbers of channels, meaning SDT is indicating there is no evidence for global processing of these stimuli unless there are a large number of channels contributing to performance.

In addition to the probability summation estimates, additive summation predictions were also calculated using SDT (although the authors have reservations about the validity of these predictions, which we explain in the Discussion section). As can be seen in Figure 10, additive summation estimates closely fit the observed data for an RF3. A four-fold observer level cross-validation (i.e., using each observer as a fold) confirmed that additive summation had a lower average RMSE (0.0014) and, therefore, provided a better explanation of the data than probability summation with a low number of channels (0.0030). For the RF5, additive summation estimates were significantly steeper than observer thresholds (assessed using visual inspection; Cumming, 2014) and cross-validation suggested probability summation estimates with a low number of channels provided the best fit for the data (0.00077), followed by additive summation

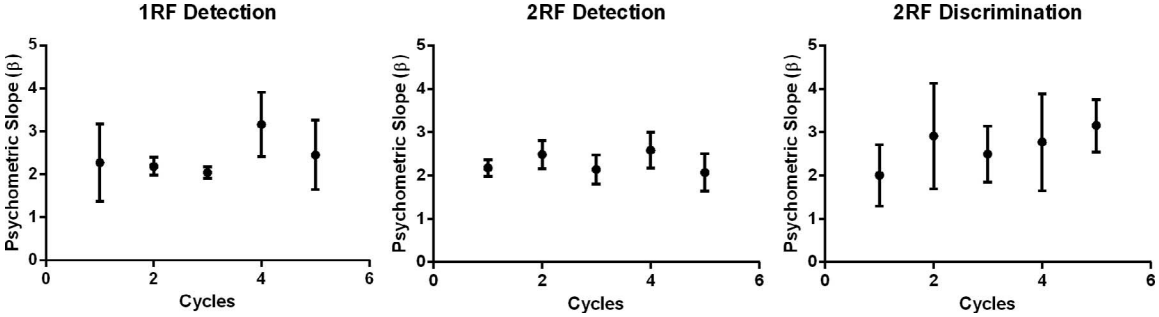

Figure 9. Average psychometric slopes of all four observers with 95% CIs across the three conditions. Again, as with the RF3 data, there appears to be no consistent pattern across the data.

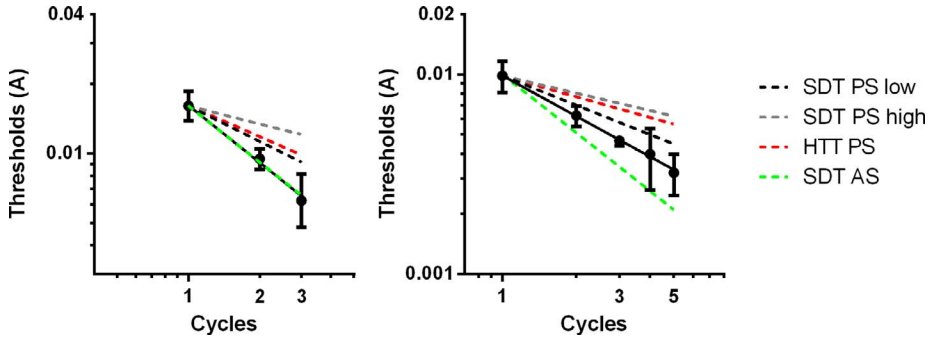

Figure 10. Average detection thresholds (black solid circles) with fitted power functions (solid line; –0.81 for RF3; and –0.68 for RF5) for the four observers with 95% CIs and probability summation estimates for HTT (red dashed line; –0.45 RF3 and –0.35 RF5), SDT with a low number of channels (black dashed line; –0.51 RF3 and –0.49 RF5), SDT with a high number of channels (gray dashed line; –0.26 RF3 and –0.29 RF5), and SDT additive summation (fixed attention window; green dashed line; –0.81 RF3 and –0.97 RF5).

(0.0013), then probability summation with a high number of channels (0.0020).

Summary

We have found evidence suggesting RF patterns with different wavelengths can be discriminated from each other at their detection thresholds when the number of cycles of modulation is greater than one. That is, we are able to make global shape judgments of RF patterns at their threshold for detection when there is more than one cycle of modulation. This is strong evidence for global processing of these patterns that is not dependent on HTT or SDT probability summation predictions and shows that local differences are poorly discriminated (i.e., at one cycle of modulation; see also Dickinson et al., 2013). We've also found evidence that having different stimuli (RF3 and RF5) within the same block produces the same detection thresholds as when the stimuli are presented by themselves. This suggests these two stimuli are independently processed, further evidence against the assumption that probability summation is supporting the measured thresholds.

Detection slope	*M*	$\sigma_{\bar{D}}$	*t*(*df*)	*p*	Cohen's *d*
RF3	0.81				
PS(1, 3)	0.51	0.27	3.35(3)	0.044*	1.68
PS(2, 6)	0.50	0.27	3.51(3)	0.039*	1.75
PS(1, 120)	0.26	0.24	6.92(3)	0.006*	3.46
PS(2, 120)	0.25	0.24	7.16(3)	0.006*	3.58
RF5	0.68				
PS(1, 5)	0.49	0.27	2.06(3)	0.131	1.03
PS(2, 10)	0.48	0.27	2.24(3)	0.111	1.12
PS(1, 72)	0.29	0.23	5.55(3)	0.012*	2.78
PS(2, 72)	0.28	0.22	5.91(3)	0.010*	2.95

Table 1. Means, standard deviations, and inferential statistics for paired-samples *t* tests comparing threshold detection slopes with the corresponding probability summation (PS) slope. *Note*: PS(x,Q) estimates were calculated for each observer at each point by using Q number of channels and x × number of cycles of modulation for number of local elements. *$p < 0.05$.

The HTT method produced probability summation estimates that were typical of previous research (Loffler et al., 2003; Wilkinson et al., 1998). Observer slopes for both patterns were steeper than those found by Baldwin et al. (2016), and the thresholds decreased significantly faster than their respective estimates of probability summation, which has typically been taken as evidence of global processing. This evidence is consistent with the conclusions arising from our data comparing detection and discrimination thresholds for these patterns, which is generated independently of HTT. SDT estimates of probability summation varied, with all probability summation slope estimates being significantly shallower than the detection slope for an RF3 but only significantly shallower for an RF5 when estimated on the assumption that the higher number of channels was relevant—numbers that seem to be warranted with random phase stimuli. Additive summation estimates approximated observer thresholds for an RF3, but were significantly steeper than observer thresholds for an RF5. Taken together, SDT estimates were able to identify integration in the strongly integrating RF3 pattern, but were less conclusive for the weaker integration of the RF5 (the implications of which are discussed below).

Discussion

The results provide strong evidence that observers were able to discriminate between RF patterns at their threshold for detection when the number of cycles of modulation was greater than one. Discrimination of the patterns would, at minimum, require the use of two points on the object's contour to make a global judgment about the pattern's shape. The authors of the

current paper believe these points to be corners (Dickinson et al., 2012), and the critical feature the polar angle subtended by separation of the corners at the center of the pattern (Dickinson et al., 2013), which is discussed below. This discrimination at threshold is evidence that the observers are integrating information along the contour of the pattern and, therefore, demonstrating global processing of RF patterns at threshold, a result supported by parallel visual search performance (Almeida et al., 2013).

SDT only rejected probability summation for RF5 patterns when the number of channels being monitored was appropriate for random phase stimuli but could also do so for RF3 with a much smaller channel estimation. Additionally, additive summation predictions seemed appropriate for RF3 patterns, but were significantly steeper than observer thresholds for an RF5. If we were purely using SDT to examine whether there was integration around the contour of an RF5, we likely would have drawn incorrect conclusions. Even though the additive summation estimates provided a better fit than the probability summation with a high number of channels, it would easily have been argued that observer data was significantly different to both predictions (assessed using visual inspection; Cumming, 2014) and that the data was inconclusive. Therefore, more investigation is required to determine the appropriate number of channels required in the accurate generation of probability summation predictions using SDT and whether the current models are able to generate appropriate additive summation estimates for RF patterns. We know for the probability summation predictions to be shallow enough to correctly reject probability summation of an RF5, the number of channels needs to be relatively high. But the exact value and whether it changes for each individual pattern is still unclear.

Although we have suggested a large number of channels is required in the correct generation of probability summation estimates, we do not believe there are a large number of channels that are monitored by the visual system when detecting deformation in low frequency RF patterns. Our results have already demonstrated strong evidence against probability summation, as observers were able to discriminate between the patterns at threshold. This suggests integration of information around the contour and furthermore, it suggests, as outlined by Watson and Robson (1981), there are independent labelled detectors for the RF3 and RF5 (i.e., in their terms there is an RF3 channel and an RF5 channel). This would suggest one channel, rather than a large number, is responsible for the processing of each RF pattern, although it does not prove it is specifically an RF channel (Dickinson et al., 2013).

Interestingly, there was no change in observer thresholds when the RF patterns were presented as blocked or interleaved (i.e., when only a single possible RF was presented within a block of trials or when both the RF3 and RF5 were presented within the same block of trials). This would suggest there is no penalty for monitoring for the presence of different RF patterns at the same time. Kingdom et al. (2015, p. 3) noted that changing from blocked to interleaved presentation should also result in changes in threshold for stimuli conforming to probability summation under SDT. Therefore, as there is no difference in thresholds between blocked and interleaved conditions, we conclude this is evidence against probability summation driving the processing of low frequency RF patterns. Furthermore, there was no evidence of psychometric slopes becoming more shallow with increasing numbers of cycles of modulation (see Figures 8 and 9), a key feature of the SDT probability summation model (Baldwin et al., 2016; Pelli, 1985). In fact, previous research examining the effect of increasing numbers of cycles of modulation on psychometric functions have also found no evidence for a decrease in the slope of the psychometric functions (Baldwin et al., 2016; Cribb, Badcock, Maybery, & Badcock, 2016), further evidence against SDT probability summation for low frequency RF patterns which again, does not rely on summation estimates.

Analysis of the data using HTT is consistent with our evidence for global shape processing, with detection thresholds decreasing faster than those predicted by probability summation. HTT, therefore, seems not to have falsely identified that global shape processing was occurring in both the RF3 and RF5 stimuli. With the current evidence from the receiver operating characteristic curves presented in Baldwin et al. (2016), we agree HTT analysis is not the most appropriate for RF patterns; however, we wished to include HTT to use as a comparison to SDT. We can see from the data that when an appropriate number of channels is used in the SDT calculation, estimates are shallower than when HTT based estimates are employed. This suggests the HTT estimates of probability summation can be more conservative than SDT and that previous researchers who used this method (along with random phase RF patterns, as most did) and found evidence of global processing, likely would have done so using SDT analysis.

Schmidtmann et al. (2012) investigated the integration of information around complete RF patterns (a pattern with a fully modulated contour; e.g., RF3) and incomplete RF patterns (where there is a portion of the contour which is an unmodulated circle; e.g., RF3[2]). They suggested that integration of information only occurs around low frequency complete RF patterns, not for incomplete RF patterns. However, the current results provide strong evidence against this suggestion, as we have demonstrated that discrimination at threshold is possible for incomplete RF patterns. Therefore, inte-

gration of information is occurring around patterns with incomplete modulation of their radius.

The difference in interpretation between the current results and those found by Schmidtmann et al. (2012) may arise from their use of a theoretical value for probability summation, rather than a value calculated from the pertinent data in their study. They chose to use a value of −0.33 for probability summation, following Loffler et al. (2003); however, research calculating probability summation typically show estimates greater than −0.33 (Bell & Badcock, 2008; Dickinson et al., 2010; Dickinson et al., 2012; Green et al., 2017; Tan et al., 2013). Perhaps these patterns, similar to those used in other studies (Baldwin et al., 2016; Mullen, Beaudot, & Ivanov, 2011), contained a salient local cue that caused a flattening of integration slopes (see Dickinson et al., 2012; and Green et al., 2017). This cue may have been created by not employing the D1 smoothing function to join the sine wave to the circular contour.

Results of the current paper revisit those of Baldwin et al. (2016) who were unable to reject either probability summation or additive summation estimates using SDT (also see Green, Dickinson, & Badcock, 2018b). Their results are most likely due to their use of fixed phase stimuli. Indeed, they acknowledge the use of fixed phase stimuli was likely the cause of their lack of improvement in detection when adding cycles of modulation to their blocked condition (with a slope of −0.18 for single RF and 0.06 for quad RF; Baldwin et al., 2016). This lack of change in detection thresholds for their blocked conditions demonstrates how locally observers can focus their attention, as it reflects a complete disregard of the increase in number of local elements. Baldwin et al. (2016) did use an interleaved condition to increase spatial uncertainty (finding a slope of −0.53 for the single RF and −0.60 for the quad RF conditions); however, we do not believe this is analogous to a random phase pattern (we found −0.81 for an RF3 and −0.68 for an RF5), as the deformation in their study could only occur in one of four known locations and thus still only requires a small number of channels to be monitored. This highlights the problem with using fixed phase stimuli when attempting to measure global processing—if the observers know where to look to detect deformation, they are not required to monitor the whole pattern. This would make it possible to use a local attentional strategy and reduce the likelihood of global processing occurring around a shape.

Similar to Baldwin et al. (2016), past research has also claimed to have found evidence against global processing of RF patterns (Mullen et al., 2011); however, like the methodology of Baldwin et al. (2016), they also created a salient local cue that observers could use for detection. Dickinson et al. (2012) showed that by removing the certainty by which this local cue location could be determined, thresholds changed and global processing of the pattern was observed. Their results were originally compared to HTT probability summation estimates; however, given this is likely a more conservative analysis and the steepness of the slopes (average of −0.81 across four observers) it is likely their RF4 thresholds would have been significantly steeper than probability summation under either method of estimation. Thus, we expect that if Baldwin et al. (2016) used random phase RF patterns (i.e., removing the spatial certainty of the deformation), they too would have obtained thresholds reflecting global shape processing for RF patterns.

As noted, discrimination at threshold required two or more cycles of modulation and suggests a critical feature appears, which is not present with only one cycle of modulation. In line with previous research (Bell et al., 2008; Bowden, Dickinson, Fox, & Badcock, 2015; Dickinson et al., 2013; Dickinson et al., 2015), we believe this critical feature to be polar angle subtended at the center of the RF between the estimated corner locations. The results of the current study support that of Dickinson et al. (2013) who also found observers were able to discriminate RF patterns with more than two cycles of modulation at their threshold for detection. Again, similar to Dickinson et al. (2013), we found that at one cycle of modulation, observers were unable to discriminate between RF patterns at the threshold for detection (see Figures 3 and 6).

To test if polar angle is the critical feature, Dickinson et al. (2013) examined detection and discrimination thresholds for differing numbers of cycles of an RF3 and an RF6. Results showed observers were able to discriminate between an RF3 with three cycles of modulation and an RF6 with six cycles of modulation at their thresholds for detection. They then tested an RF6 with three adjacent cycles of modulation and an RF6 with six cycles of modulation. As both patterns have the same polar angle between nearest corners, but differing number of cycles, it would be expected that observers would be unable to discriminate between the patterns at detection threshold if polar angle was the cue (this assumes the outer polar angle does not affect discrimination). This is exactly what they found. Furthermore, when they tested discrimination and detection thresholds for an RF3 with three cycles of modulation and an RF6 with only every second cycle of modulation present (i.e., it approximated the polar separation of an RF3, but the cycles of modulation were half the wavelength), they found observers were unable to discriminate between these patterns at threshold. Therefore, there is strong evidence that the

critical feature in discriminating between RF patterns at threshold is polar angle.

Although detection at threshold for discrimination requires two or more cycles of modulation, it is not evidence that global shape processing only occurs when two or more cycles are present. The discrimination task is a task that requires a global judgment to be made. This judgment appears to be greatly affected by the presence of an internal polar angle (as demonstrated by Dickinson et al., 2013). Once this cue is available, the judgment can be made at the threshold for detection, providing evidence that observers are able to see the global shape and, therefore, global shape processing is occurring. The inability to discriminate between RF patterns with one cycle of modulation is not evidence of a lack of global processing. The authors of the current study still maintain that integration of information around the pattern's contour occurs regardless of the number of cycles of modulation, and therefore, an observer's threshold at one cycle of modulation is a valid data point when estimating that observer's strength of integration but it is insufficient to identify the particular RF pattern.

Conclusion

Results of the current study support previous research suggesting low frequency RF patterns are globally processed. Analysis of data using HTT was consistent with these results, suggesting use of this method may not have distorted the conclusions obtained with previous RF pattern data. SDT is a more appropriate method; however, it appears that further work is required to determine the appropriate number of channels required for both probability and additive summation calculations to produce accurate estimates for RF patterns. The evidence for global integration of contour information is therefore still compelling.

Keywords: shape perception, global processing, signal detection theory, RF patterns, probability summation, discrimination at threshold

Acknowledgments

The research was supported by Australian Research Council grants DP110104553 and DP160104211 to DRB and a University Postgraduate Award scholarship to RJG. Thanks to Jonathan Patrick and Margaret Bowden. Also, a very big thanks to Daisy Phillips.

Commercial relationships: none.

Corresponding author: Robert J. Green.
Email: robert.green@research.uwa.edu.au.
Address: School of Psychological Science, The University of Western Australia, Perth, Australia.

References

Almeida, R. A., Dickinson, J. E., Maybery, M. T., Badcock, J. C., & Badcock, D. R. (2010a). A new step towards understanding Embedded Figures Test performance in the autism spectrum: The radial frequency search task. *Neuropsychologia*, *48*(2), 374–381, https://doi.org/10.1016/j.neuropsychologia.2009.09.024.

Almeida, R. A., Dickinson, J. E., Maybery, M. T., Badcock, J. C., & Badcock, D. R. (2010b). Visual search performance in the autism spectrum II: The radial frequency search task with additional segmentation cues. *Neuropsychologia*, *48*(14), 4117–4124.

Almeida, R. A., Dickinson, J. E., Maybery, M. T., Badcock, J. C., & Badcock, D. R. (2013). Visual search targeting either local or global perceptual processes differs as a function of autistic-like traits in the typically developing population. *Journal of Autism and Developmental Disorders*, *43*(6), 1272–1286.

Almeida, R. A., Dickinson, J. E., Maybery, M. T., Badcock, J. C., & Badcock, D. R. (2014). Enhanced global integration of closed contours in individuals with high levels of autistic-like traits. *Vision Research*, *103*, 109–115, https://doi.org/10.1016/j.visres.2014.08.015.

Baldwin, A. S., Schmidtmann, G., Kingdom, F. A., & Hess, R. F. (2016). Rejecting probability summation for radial frequency patterns, not so Quick! *Vision Research*, *122*, 124–134, https://doi.org/10.1016/j.visres.2016.03.003.

Bell, J., & Badcock, D. R. (2008). Luminance and contrast cues are integrated in global shape detection with contours. *Vision Research*, *48*(21), 2336–2344, https://doi.org/10.1016/j.visres.2008.07.015.

Bell, J., Badcock, D. R., Wilson, H., & Wilkinson, F. (2007). Detection of shape in radial frequency contours: Independence of local and global form information. *Vision Research*, *47*(11), 1518–1522.

Bell, J., Dickinson, J. E., & Badcock, D. R. (2008). Radial frequency adaptation suggests polar-based coding of local shape cues. *Vision Research*, *48*(21), 2293–2301.

Bowden, V. K., Dickinson, J. E., Fox, A. M., &

Badcock, D. R. (2015). Global shape processing: A behavioral and electrophysiological analysis of both contour and texture processing. *Journal of Vision*, *15*(13):18, 1–23, https://doi.org/10.1167/15.13.18. [PubMed] [Article]

Cribb, S. J., Badcock, J. C., Maybery, M. T., & Badcock, D. R. (2016). Dissociation of local and global contributions to detection of shape with age. *Journal of Experimental Psychology: Human Perception and Performance*, *42*(11), 1761–1769, https://doi.org/10.1037/xhp0000257.

Cumming, G. (2014). The new statistics: Why and how. *Psychological Science*, *25*(1), 7–29, https://doi.org/10.1177/0956797613504966.

Dickinson, J. E., Bell, J., & Badcock, D. R. (2013). Near their thresholds for detection, shapes are discriminated by the angular separation of their corners. *PLoS One*, *8*(5), e66015, https://doi.org/10.1371/journal.pone.0066015.

Dickinson, J. E., Cribb, S. J., Riddell, H., & Badcock, D. R. (2015). Tolerance for local and global differences in the integration of shape information. *Journal of Vision*, *15*(3):21, 1–24, https://doi.org/10.1167/15.3.21. [PubMed] [Article]

Dickinson, J. E., Haley, K., Bowden, V. K., & Badcock, D. R. (2018). Visual search reveals a critical component to shape. *Journal of Vision*, *18*(2):2, 1–25. https://doi.org/10.1167/18.2.2. [PubMed] [Article]

Dickinson, J. E., Han, L., Bell, J., & Badcock, D. R. (2010). Local motion effects on form in radial frequency patterns. *Journal of Vision*, *10*(3):20, 1–15. [PubMed] [Article]

Dickinson, J. E., McGinty, J., Webster, K. E., & Badcock, D. R. (2012). Further evidence that local cues to shape in RF patterns are integrated globally. *Journal of Vision*, *12*(12):16, 1–17, https://doi.org/10.1167/12.12.16. [PubMed] [Article]

Graham, N. V. S. (1989). *Visual pattern analyzers*. New York, NY: Oxford University Press.

Green, R. J., Dickinson, J. E., & Badcock, D. R. (2017). Global processing of random-phase radial frequency patterns but not modulated lines. *Journal of Vision*, *17*(9):18, 1–11, https://doi.org/10.1167/17.9.18. [PubMed] [Article]

Green, R. J., Dickinson, J. E., & Badcock, D. R. (2018a). The effect of spatiotemporal displacement on the integration of shape information. *Journal of Vision*, *18*(5):4, 1–18, https://doi.org/10.1167/18.5.4. [PubMed] [Article]

Green, R. J., Dickinson, J. E., & Badcock, D. R. (2018b). Integration of shape information occurs around closed contours but not across them. *Journal of Vision*, *18*(5):6, 1–13, https://doi.org/10.1167/18.5.6. [PubMed] [Article]

Kingdom, F. A., Baldwin, A. S., & Schmidtmann, G. (2015). Modeling probability and additive summation for detection across multiple mechanisms under the assumptions of signal detection theory. *Journal of Vision*, *15*(5):1, 1–16, https://doi.org/10.1167/15.5.1. [PubMed] [Article]

Kingdom, F. A., & Prins, N. (2010). *Psychophysics: A practical introduction*. London, UK: Elsevier.

Loffler, G., Wilson, H. R., & Wilkinson, F. (2003). Local and global contributions to shape discrimination. *Vision Research*, *43*(5), 519–530.

Mullen, K. T., Beaudot, W. H. A., & Ivanov, I. V. (2011). Evidence that global processing does not limit thresholds for RF shape discrimination. *Journal of Vision*, *11*(3):6, 1–21, https://doi.org/10.1167/11.3.6. [PubMed] [Article]

Pelli, D. G. (1985). Uncertainty explains many aspects of visual contrast detection and discrimination. *Journal of the Optical Society of America, A*, *2*(9), 1508–1532.

Prins, N., & Kingdom, F. A. A. (2009). *Palamedes: Matlab routines for analyzing psychophysical data*. Retrieved from http://www.palamedestoolbox.org.

Quick, R. F. (1974). A vector-magnitude model of contrast detection. *Kybernetik*, *16*(2), 65–67, https://doi.org/10.1007/bf00271628.

Schmidtmann, G., Jennings, B. J., Bell, J., & Kingdom, F. A. (2015). Probability, not linear summation, mediates the detection of concentric orientation-defined textures. *Journal of Vision*, *15*(16):6, 1–19, https://doi.org/10.1167/15.16.6. [PubMed] [Article]

Schmidtmann, G., Kennedy, G. J., Orbach, H. S., & Loffler, G. (2012). Non-linear global pooling in the discrimination of circular and non-circular shapes. *Vision Research*, *62*, 44–56.

Tan, K. W., Dickinson, J. E., & Badcock, D. R. (2013). Detecting shape change: Characterizing the interaction between texture-defined and contour-defined borders. *Journal of Vision*, *13*(14):12, 1–16, https://doi.org/10.1167/13.14.12. [PubMed] [Article]

Van Essen, D. C., Anderson, C. H., & Felleman, D. J. (1992, January 24). Information processing in the primate visual system: An integrated systems perspective. *Science*, *255*(5043), 419.

Vernon, R. J., Gouws, A. D., Lawrence, S. J., Wade, A. R., & Morland, A. B. (2016). Multivariate patterns in the human object-processing pathway reveal a shift from retinotopic to shape curvature representations in lateral occipital areas, LO-1 and LO-2. *Journal of Neuroscience*, *36*(21), 5763–5774.

Watson, A. B., & Robson, J. G. (1981). Discrimination at threshold: Labelled detectors in human vision. *Vision Research*, *21*(7), 1115–1122.

Westheimer, G. (1976). Diffraction theory and visual hyperacuity. *Optometry & Vision Science*, *53*(7), 362–364.

Westheimer, G. (2010). Visual acuity and hyperacuity. *The Optical Society of America Handbook of Optics. Volume III*. New York, NY: McGraw-Hill.

Wilkinson, F., Wilson, H. R., & Habak, C. (1998). Detection and recognition of radial frequency patterns. *Vision Research*, *38*(22), 3555–3568.

Wilson, H. R. (1980). A transducer function for threshold and suprathreshold human vision. *Biological Cybernetics*, *38*(3), 171–178.

Wilson, H. R., & Propp, R. (2015). Detection and recognition of angular frequency patterns. *Vision Research*, *110*, 51–56.